Text and references to accompany Nevada Bureau of Mines and Geology Map 132

STRUCTURAL EVOLUTION OF THE WHITE HORSE PASS AREA

SOUTHEAST ELKO COUNTY, NEVADA

by

N.J. Silberling and K.M. Nichols

INTRODUCTION

The White Horse Pass map area includes the White Horse Pass 7.5′ Quadrangle and adjacent parts of the White Horse Mountain, Goshute Peak, Ferguson Mountain, and Kinsley Mountains 7.5′ Quadrangles (fig. 1). Bedrock within this area crops out in the southern part of the main Goshute Mountains, the White Horse Mountain massif, the Ferguson Hills in the northeast part of the map area, and the Ferber Hills in the southeast part of the map area. These topographically elevated areas surround the White Horse Flat pediment, which covers the central part of the White Horse Pass Quadrangle and the southern part of the Ferguson Mtn. Quadrangle. Along the eastern edge of the map area, lacustrine deposits of Pleistocene Lake Bonneville lap onto older Quaternary gravels covering the pediment surface. Highstand deposits of another Pleistocene lake that occupied the Antelope and Goshute valleys also occur along the west side of the map area.

Pre-Tertiary stratified rocks of the White Horse Pass area range from Late Devonian to Early Triassic in age. The older and younger parts of this succession are separated by a major east-rooted Tertiary extensional detachment fault referred to herein as the Ferguson detachment. In the map area this detachment is located at the stratigraphic level of the Mississippian Chainman Shale. Mississippian and older strata that are mostly gently dipping are exposed in the footwall, and the hanging wall is composed of Pennsylvanian and younger strata, which dip moderately to steeply to the west, or are even overturned. The hanging wall of this detachment—termed here the Ferguson detachment—has been previously referred to as the "Ferguson Mountain terrane" by Ketner (1997; Ketner and others, 1998) and to "structural plates 3 and 4" by Welsh (1994) who regarded these "plates" as Middle Jurassic tectonic features. Strongly tilted Tertiary volcanic and sedimentary rocks are included in the hanging wall of the detachment (fig. 1) and attest to its Cenozoic age. The hanging wall of the Ferguson detachment is disrupted by numerous faults which are cut by the detachment or merge into it, as well as by post-detachment normal faults. The Ferguson detachment and its hanging wall provide a well-exposed sample of a much larger, east-rooted, Tertiary detachment system (Ketner and others, 1998), that extends at least as far north as the Toano Range and Leppy Hills and as far east as the northern Deep Creek Range in Utah. This fault system appears to be a shallow-level expression and northern continuation of the Snake Range-Deep Creek Range fault system of (Miller and others, 1999), which characterizes ranges farther south in central eastern Nevada.

Folded and faulted Devonian and Mississippian strata intruded by a late Middle or early Late Jurassic pluton—the White Horse pluton—are exposed in the footwall of the Ferguson detachment. Devonian strata surrounding the pluton are isoclinally folded and contact metamorphosed. The geology of the footwall bears on important problems in pre-Tertiary Great Basin geology. Among these, the succession and timing of distinct generations of Mesozoic deformation in this area provide a link between the Mesozoic structural histories of ranges to the east (such as the northern Deep Creek Range) and those farther west (such as the Cherry Creek and Pequop Ranges). Also of importance and exceptionally well displayed in the map area are Mesozoic attenuation faults (Hintze, 1978; Thorman and others, 1994) that can be related to the White Horse pluton and to other Mesozoic structures in the map area (Silberling and Nichols, 1994). Recognition and interpretation of attenuation faulting affecting the Mississippian-Devonian record here is critical to paleogeographic and palinspastic reconstruction of the Devonian-Mississippian Antler foreland (Silberling and others, 1997). The stratigraphic record of foreland strata in the area was previously misinterpreted by Silberling and others (1995) because of the structural omission of strata by attenuation faults.

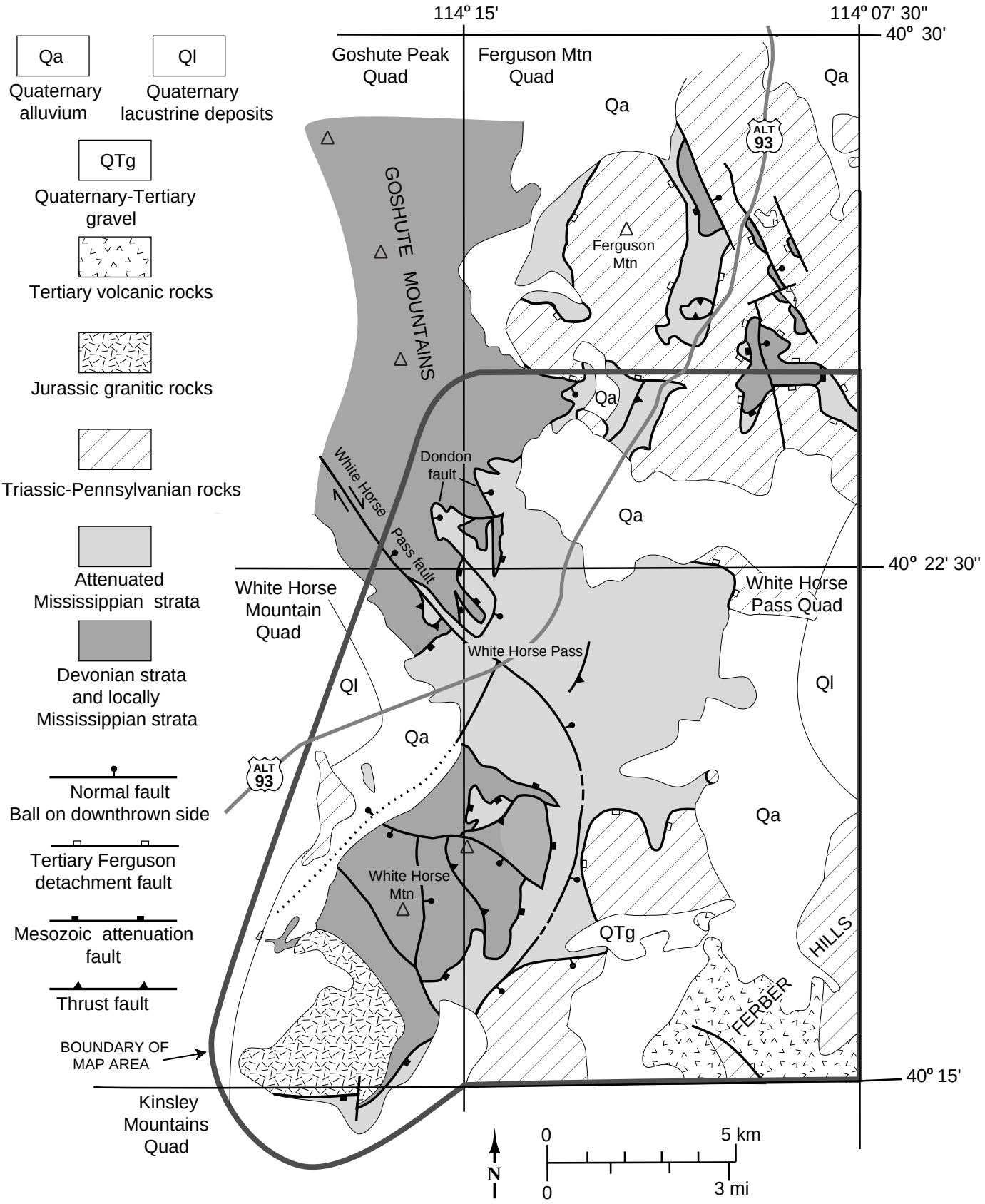

Figure 1. Index map locating the map area in relation to the White Horse Pass 7.5' Quadrangle and adjoining quadrangles and showing some of the principal geographic and geologic features. Geology within Ferguson Mtn. Quadrangle modified after Welsh (1994).

MESOZOIC STRUCTURE

Structural features, including folds and thrust faults, that deform the pre-Tertiary strata of the White Horse Pass area belong to three generations of deformation, D_1, D_2, and D_3. Each phase of deformation is represented by a unique set of structures and is discussed sequentially below.

D_1 Structures

D_1 structures include attenuation faults and the isoclinal folds that are geometrically associated with the margin of the ca. 160 Ma (Armstrong, 1970; Miller and Hoisch, 1995) White Horse pluton and are interpreted to be syn-plutonic. In addition, widespread bedding-parallel solution(?) cleavage within the White Horse Pass limestone member of the Chainman Shale (Mcw) is folded and faulted by D_2 structures and is thus also interpreted as a D_1 feature resulting in part from regional heating during pluton emplacement. At the outset of Mesozoic deformation the maximum stratigraphic depth to the top of the Devonian in the area is estimated at only about 4 to 5 km, but conodont alteration indices (CAI's) in Mississippian strata from the vicinity of White Horse Pass are about 5 (Karklins and others, 1989; R.G. Stamm, written commun., 1994), interpreted to represent heating to temperatures of ca. 300° C (Epstein and others, 1977). This would have far exceeded heating resulting from the normal geothermal gradient and thus is ascribed to the late Middle to early Late Jurassic period of regional magmatism in the northeastern Great Basin (Miller, 1990) that included intrusion of the White Horse pluton.

The Guilmette Formation (Dg) in the metamorphic aureole of the White Horse pluton contains spectacular tight to isoclinal map-scale (F_1) folds, attention to which was first drawn by Misch (1960). The pluton intrudes the upright limb of a largely overturned, inward-facing syncline whose axis wraps around and conforms to the roughly circular pluton margin. This fold and the more outward, coordinate, major anticline can be traced for more than a third of the way around the pluton; metamorphic lineations, defined by stretching of mineral grains and fossils parallel to the foliation within the sheared F_1 fold limbs, are crudely radial to the pluton margin. These F_1 folds and the associated metamorphic fabrics are thus clearly the localized result of ascending pluton emplacement, as pointed out by Allmendinger and Miller (1991). Although intrusion of this pluton profoundly deformed its wall rocks, internally it lacks structural fabric other than a spaced cleavage along its southwest edge, which may be related to subsequent (F_3?) folding.

Attenuation faults within the Mississippian succession can also be related to the time of emplacement of the White Horse pluton. Approaching the pluton, the structurally and stratigraphically lowest attenuation fault gradually cuts down section from a level in the basal part of the Needle Siltstone Member of the Chainman Shale (Mcn) to a level within the upper member of the Joana Limestone (Mju)—a stratigraphic separation of only a few tens of meters—from north to south along the east flanks of the White Horse Mountain massif and the main Goshute Range over a distance of about 13 km. A higher attenuation fault separates the White Horse Pass limestone member of the Chainman Shale (Mcw) from underlying units near the White Horse pluton and also in the northern part of map area. In proximity to the pluton the higher of these attenuation faults truncates the hanging wall of the lower attenuation fault. The highest of the recognized attenuation faults has as its hanging wall throughout the map area the argillite member of the Chainman Shale (Mca), which in different places is separated by this fault from various underlying units ranging from the siltstone member of the Chainman (Mcs) down to the Guilmette Formation (Dg). A swarm of sills, usually much altered but originally of granitic texture and intermediate composition, occurs in the lowest part of the Chainman argillite (Mca), following the attenuation fault from the vicinity of the White Horse pluton to as far as several kilometers northeast of White Horse Pass. Some of these sills also intrude the structurally highest footwall rocks of this attenuation fault. These isotopically undated sills range from less than a meter to several meters in thickness, and most of them are too thin to be shown individually on the geologic map. Like the attenuation fault with which they are associated, they are apparently folded and faulted by D_2 structures.

As portrayed diagrammatically in figure 2, upon approaching the White Horse pluton from the north, the attenuation faults overstep one another so that the Chainman

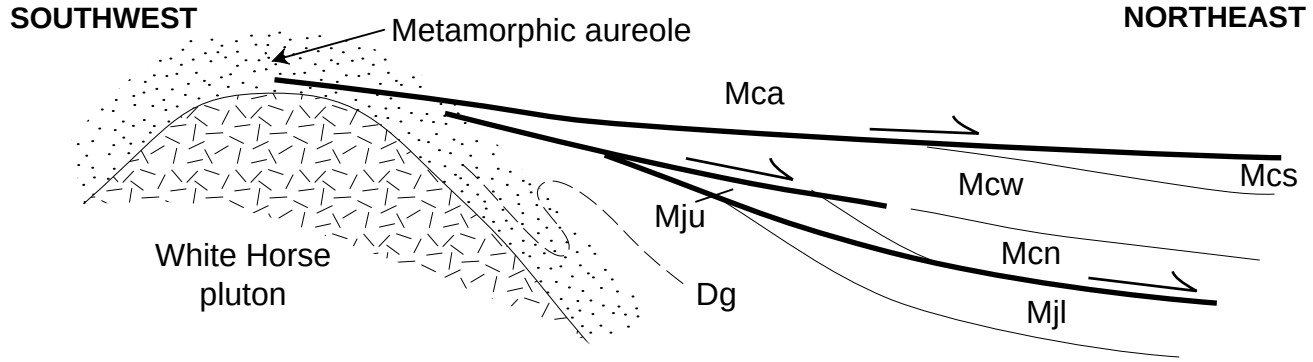

Figure 2. Schematic cross section showing the relationships among the attenuation faults and stratigraphic units as they are traced southwestward toward the White Horse pluton. This pattern is interpreted to be the result of progressive tilting of strata and gravity-driven faulting in response to thermal uplift associated with pluton emplacement.

argillite eventually comes in contact, or nearly so, with the pluton and is contact metamorphosed by it. The White Horse pluton crops out at the southeast end of a pronounced broad, linear, positive magnetic anomaly extending west-northwestward for about 40 km (Ponce, 1994). Another late Middle Jurassic pluton, the Melrose pluton, for which a discordant U-Pb age of ca. 165 Ma is reported by Zamudio and Atkinson (1992), crops out in the Dolly Varden Mountains near the western end of this anomaly. Although no kinematic indicators are associated with the attenuation faults, the pattern of attenuation faulting in relation to the aeromagnetically delineated plutonic trend suggests sliding off of the flanks of a growing thermal uplift. As a generalization, widespread attenuation faulting in the eastern Great Basin (Hintze, 1978; Thorman and others, 1994) may have resulted from thermal doming of relatively flat-lying strata prior to regional compressional deformation.

For interpreting the stratigraphic record of the Antler foreland, one effect of attenuation faulting in the map area is to partly eradicate the Joana Limestone from the stratigraphic succession. The resulting stratigraphic omission, and the extensive, nearly bedding-parallel, cryptic nature of the fault responsible for this, produces a pattern easily misinterpreted as the primary result of syndepositional uplift such as by a flexural peripheral bulge in the foreland. Other stratigraphic omissions produced by attenuation faulting within the Mississippian strata of the Antler foreland in the map area are also apparent from the map pattern. Nevertheless, the absence in the stratigraphic section of the Late Devonian Pilot Shale is evidently not structurally controlled, because the contact between the Joana Limestone and the Guilmette Formation, the units that bracket the Pilot in ranges to the north and to the south and southwest, is clearly depositional where well exposed in the map area (see map explanation).

The different effects of D_1 in the White Horse Pass area generally conform to the characterizations of Jurassic tectonism and magmatism in the northeastern Great Basin by Elison (1995) and Miller and Hoisch (1995) whereby superimposed extensional and compressive structures resulted from the intrusion of discrete plutons through a crust that was undergoing little tectonic thickening.

D_2 Structures

D_2 contractional structures of mesoscopic to kilometric scales are pervasive in the pre-Tertiary strata of the White Horse Pass area, and they control the general map pattern of the footwall of the Ferguson detachment. F_2 folds associated with D_2 deformation range from open and upright to close and oversteepened, or even overturned, verging to the east-northeast. Axes of minor F_2 folds plunge shallowly to about N20°W or S20°E, and the general F_2 fold axis derived from bedding attitudes within the White Horse Pass limestone member of the Chainman Shale (Mcw), lower member of the Joana Limestone (Mjl), and Guilmette Formation (Dg) in the 20 km^2 area surrounding White Horse Pass is nearly horizontal and trends about N20°W (fig. 3). In summary, F_2 fold axes in the footwall of the Ferguson detachment trend about N20°W and have shallow to negligible plunges.

Minor D_2 thrust faults include those involving the White Horse limestone (Mcw) and Needle Siltstone (Mcn) members of the Chainman Shale in the axial part of the major F_2 syncline in the S½ sec. 31, T29N,R69E and that carrying the Guilmette Limestone over the Needle Siltstone in the NE¼ sec. 26, T29N,R68E. Another style of D_2 faulting within the evenly bedded White Horse limestone might be prevalent but can only be observed in exceptional cut-bank exposures such as in the W½ sec. 33, T29N,R69E. Here, an eastward-overturned anticline overlies a west-dipping thrust that ramps up to a regionally bedding-parallel roof thrust. In a similar, smaller scale example in the SE¼ sec. 18, T29N,R69E, the ramp fault is limited by both floor and roof, bedding-parallel faults. Bedding-parallel D_2 shearing of this kind may be widespread.

Subparallel, roughly planar, steeply dipping calcite veins are conspicuous in Mcw and older carbonate units, particularly in the Mcw where they occur locally in swarms. In most places they strike about N20°W and are axial planar to the F_2 folds. In a few places they bisect the extension direction within conjugate en echelon calcite gash arrays, showing that the planar veins are extensional features (fig. 4). Consequently, the axial-planar veins are interpreted to be the result of flexural extension during folding.

D_3 Structures

D_3 contractional structures are more localized than D_2 structures and involve east-dipping faults such as the Sugar Loaf thrust, near Sugar Loaf Peak in the White Horse Mountain massif, and other well-exposed or inferred minor thrust or reverse faults, as in the W½ sec. 4 and E½ sec. 5, T29N,R69E (cross section A–A′) and the S½ sec. 29, T29N,R69E. Associated with these faults are west-northwest-vergent folds whose axes trend about N30°E. (fig. 5). The relationship between D_3 structures having this orientation and the more ubiquitous D_2 contractional structures is difficult to demonstrate in these generally low-strain rocks. However, the Sugar Loaf thrust truncates a map-scale F_2 anticline about 2 km northeast of Sugar Loaf Peak. Where a localized well-developed foliation cuts across bedding, as in sec. 27, T29N,R69E, both bedding and the crosscutting foliation are folded around an apparent F_3 axis (fig. 6), but the structural generation of this foliation is uncertain.

Locally, planar veins and related gash arrays like those associated with F_2 folds, but oriented so as to express flexural extension related to F_3 folds, are found in Mcw and still older carbonate rocks in the vicinity of F_3 folds (fig. 7)

Dondon Fault

The Dondon[1] low-angle fault north of Wild Horse Pass offsets D_1 attenuation faults. In addition, it carries a down-to-the-west, partly east-dipping fault in its hanging wall. The geometry of this fault within the hanging wall of the Dondon fault suggests that it could be a D_3 structure, and thus the Dondon may be a late or post-D_3 structure. On the

[1] "Dondon Pass" is the name used in the King Survey (Hague and Emmons, 1877, Folio Map IV) for White Horse Pass.

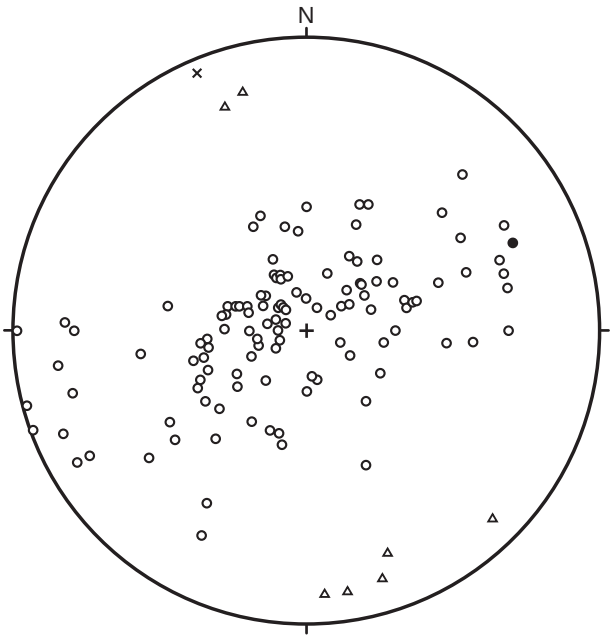

Figure 3. Stereographic projection of bedding attitudes and fold axes associated with northeast-vergent F_2 minor folds in the White Horse Pass limestone member of the Chainman Shale, the lower member of the Joana Limestone, and the Guilmette Formation in the roughly 20 km^2 area centered on White Horse Pass. *Open circles*, poles to upright bedding; *filled circle*, pole to overturned bedding; *triangles*, measured fold axes; *x*, fold axis computed from bedding.

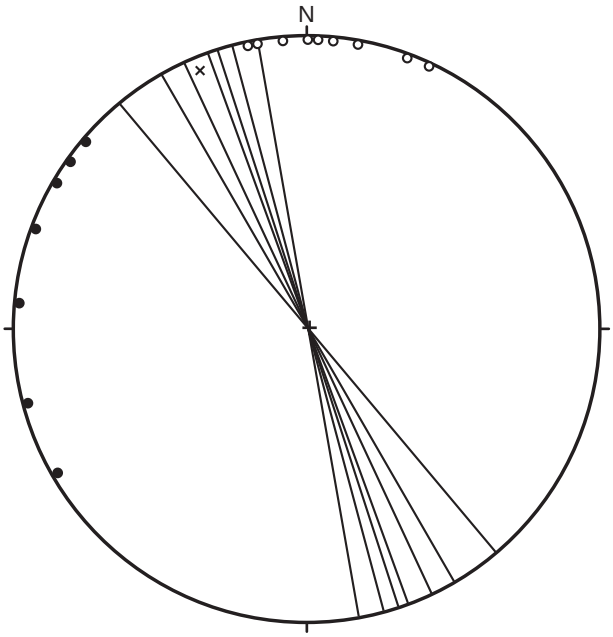

Figure 4. Two-dimensional plot showing the trends on bedding surfaces of planar calcite veins and vein sets (lines) associated with F_2 minor folds and the azimuths on bedding surfaces of associated left-slip (open circles) and right-slip (filled circles) en-echelon calcite gash arrays in the White Horse Pass limestone member of the Chainman Shale in the area immediately north of White Horse Pass. The F_2 axis computed from bedding is plotted stereographically as an *x*. The planar veins are approximately axial planar to F_2 folds, and the extension direction derived from the associated en-echelon gash arrays is perpendicular to the axial-planar veins. Both the axial-planar veins and gash arrays are therefore interpreted as flexural-extension features.

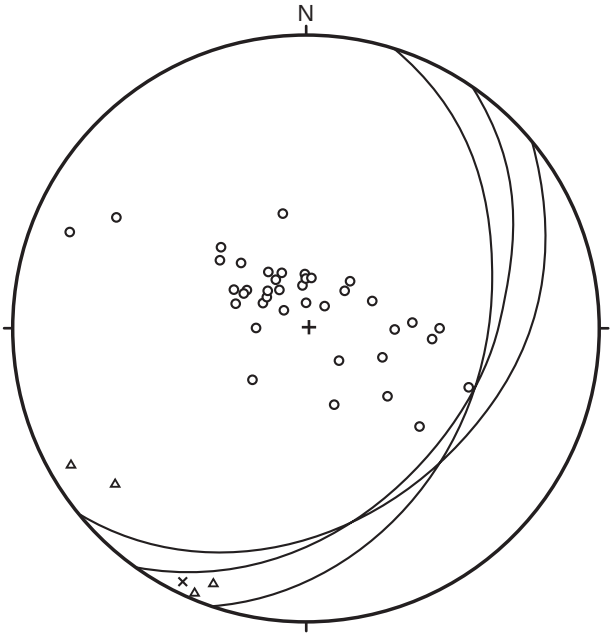

Figure 5. Stereographic projection of bedding attitudes and structural features associated with northwest-vergent F_3 minor folds in the White Horse Pass limestone member of the Chainman Shale, the lower member of the Joana Limestone, and the Guilmette Formation, which in part are directly associated with observed or inferred east-dipping thrust faults. *Open circles*, poles to bedding; *triangles*, measured fold axes; *x*, fold axis computed from bedding; *great circles*, axial-planar fracture cleavage.

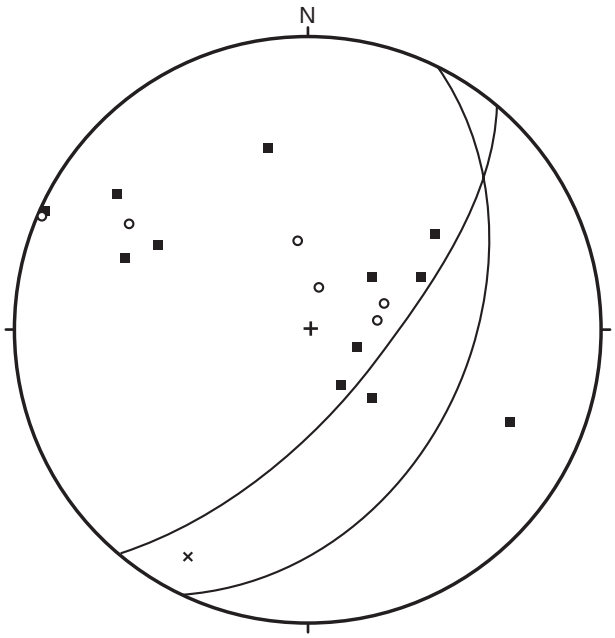

Figure 6. Stereographic projection of bedding attitudes and structural features associated with northwest-vergent F_3 folds in the limestone of White Horse Pass 5 to 6 km east of White Horse Pass (sec. 27, T29N,R69E). *Open circles*, poles to bedding; *filled squares*, poles to foliation; *x*, fold axis computed from bedding and foliation; *great circles*, spaced fracture cleavage.

other hand, the map trace of the Dondon fault suggests that it is folded by northwest-trending F_2 folds, making it a D_1 structure. In any case, the Dondon fault is younger than the structurally lower of the D_1 attenuation faults and older than the Tertiary Ferguson detachment, which cuts across it at the north margin of the map area. Granitic dikes of unknown age intermittently parallel and locally intrude the trace of the Dondon fault on the east flank of the main Goshute Range 4 to 7 km north of White Horse Pass. The transport direction on the Dondon fault is uncertain, but the outcrop pattern in its hanging wall in secs. 13 and 24, T29N,R68E suggests down-to-the-southwest tilting corresponding to northeastward transport. Strata in the hanging wall of the Dondon fault are more obviously discordant with their footwall rocks than are those associated with D_1 attenuation faults. However, map relations are inadequate to show whether or not the upper attenuation fault carrying the Chainman argillite (Mca) is cut by the Dondon fault. If this fault is a D_1 structure, the upper attenuation fault could conceivably carry the Chainman argillite over both the footwall and hanging wall of the Dondon low-angle fault, all of these structures being part of a continuum of thermal uplift and gravitational sliding.

Summary

In summary, the oldest Mesozoic deformation, D_1 is associated with emplacement of the ca. 160 Ma (Armstrong, 1970; Miller and Hoisch, 1995) White Horse pluton. Isoclinal F_1 folds in the wall rocks of the pluton are related to its emplacement. Thermal doming along a plutonic trend, of which the White Horse pluton is a part, resulted in D_1 gravity-driven attenuation faulting concomitant with the metamorphism and folding around the pluton margin. Widespread bedding-parallel foliation in the White Horse limestone also formed at this time, because east-northeast-vergent F_2 folds and thrust faults deform both this foliation as well as the attenuation faults. East-directed thrusting and related structures in the Gold Hill district, about 35 km east of White Horse Pass, in the northern Deep Creek Range predate a granodiorite having K-Ar ages from biotite of about 152 Ma (Robinson, 1993; Stacey and Zartman, 1978), and these structures may be an expression of D_2 deformation in the White Horse Pass area. Comparing this K-Ar date for the pluton at Gold Hill with that of ca. 158 Ma for the White Horse Pluton, D_2 structures may be bracketed in age by the Gold Hill and White Horse plutons and thus could be a late episode of a really extensive, east-vergent contraction along the southeast margin of the late Middle to early Late Jurassic magmatic belt in the northeastern Great Basin. However, the ages of the relevant plutons need reaffirmation using now-available isotopic methods more applicable to plutonic rocks.

Subsequent D_3 west-directed thrusting and associated F_3 folds in the White Horse Pass area may relate to west-vergent structures in ranges to the west of the Goshute Range such as the Spruce Mountain syncline about 40 km northwest of White Horse Pass (Coats, 1987) and the conspicuous, approximately N30°E-trending, minor folds in Mississippian strata of the Cherry Creek Range about 55 km southwest of White Horse Pass (N.J. Silberling and K.M. Nichols, unpublished data). The ages of these structures are unconstrained within the late Mesozoic.

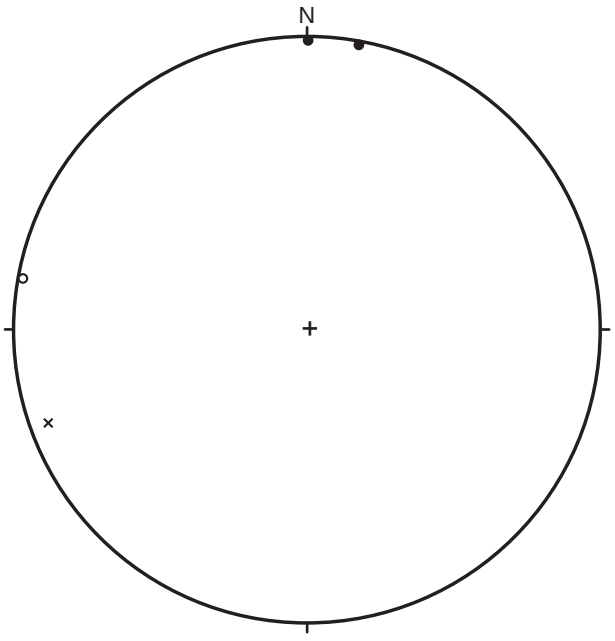

Figure 7. Two-dimensional plot showing the azimuths on bedding surfaces of left-slip (*open circle*) and right-slip (*filled circles*) en-echelon calcite gash arrays associated with a F_3 minor fold in the Guilmette Formation about 3 km west-northwest of White Horse Pass. The F_3 axis computed from bedding is plotted stereographically as an *x*.

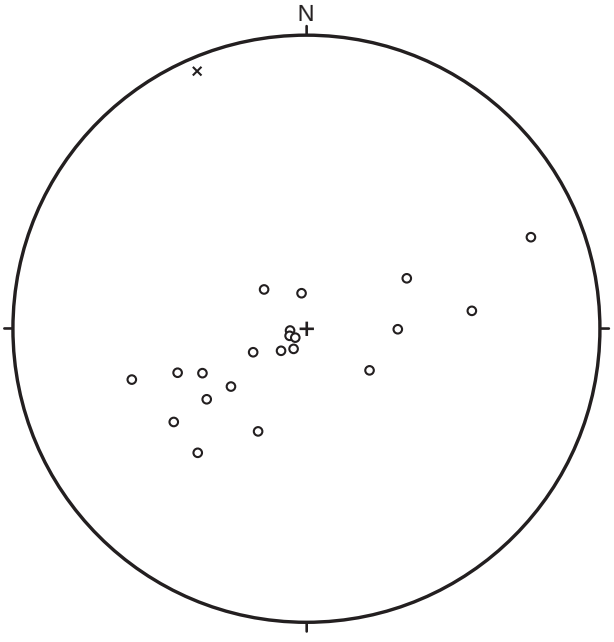

Figure 8. Stereographic projection of restored bedding attitudes (*open circles*) of the Ely Limestone and Permian unit A east of Sugar Loaf Peak (in the SE¼ sec. 8, SW¼ sec. 9, and NE¼ sec. 17, T28N,R69E). Corrected for Tertiary tilt using a rotation of 90° around a horizontal tilt axis trending 350°. *x*, fold axis computed from these restored bedding attitudes.

The low-angle Dondon fault in the White Horse Pass area could be an early Tertiary structure but more likely resulted from extensional collapse of orogenic highlands produced by late Mesozoic deformation. Unfortunately, isotopic ages are not available for the granitic dike rocks that follow the trace of the Dondon fault.

CENOZOIC STRUCTURE

Cenozoic structural features of the White Horse Pass area include the Ferguson detachment and subsequent basin-and-range normal faults. The hanging wall of the Ferguson detachment originally blanketed the entire map area. Pre-Tertiary rocks forming the hanging wall are mainly Permian strata along with more limited exposures of the Pennsylvanian Ely Limestone and one small occurrence (in north-central sec. 4, T29N,R69E) of the Lower Triassic Thaynes Formation. Within the map area, Tertiary rocks are found only in the hanging wall of the Ferguson detachment in the Ferber Hills in the southeast corner of the map where they unconformably overlie Permian strata.

In general, rocks in the hanging wall of the Ferguson detachment dip moderately to steeply west, suggesting top-to-the-east structural transport. However, much local variation in dip exists owing to pre-Tertiary folding and to dismembering of the hanging wall by high-angle faults that are confined to the detachment plate. North- to northwest-striking subsidiary normal faults in the hanging wall are mainly down-to-the-east, although some have the opposite sense of displacement. "Structural plates 3 and 4" of Welsh (1994) apparently correspond respectively to the hanging wall and footwall of these normal faults that root into the Ferguson detachment, so that either the Pennsylvanian Ely Limestone or the younger strata of Permian age may be floored by the Ferguson detachment (cross section B–B′). Still other faults confined to the hanging wall of the Ferguson plate are orthogonal to the northerly trending normal faults and both intersect and are cut by them. Some of these generally northeast- to east-trending structures may be tear faults paralleling the principal transport direction of the Ferguson detachment. Others, however, have moderate to low dips and may be normal faults responsible in part for abrupt, but small changes in bedding strikes within adjoining fault blocks, resulting from relatively minor northward or southward tilt of previously west-tilted fault blocks.

Broad pre-Tertiary folds are a more important cause of variation in the attitude of bedding in upper Paleozoic rocks in the hanging wall of the Ferguson detachment. For example, in the two coherent blocks of Ely Limestone and Permian unit A to the east of Sugar Loaf Peak in secs. 8 and 9, T28N,R69E bedding has the peculiar aspect of varying about vertical, from upright and dipping moderately west to overturned and dipping east (cross section B–B′). Although the trend of the Tertiary axis of tilt and the amount of tilt are both uncertain, restored to their pre-tilt orientation using the average attitude of Tertiary strata on the Ferguson detachment plate farther to the southeast, these upper Paleozoic rocks appear to be gently folded around a F_2 fold axis (fig. 8). Restoring original bedding attitudes of other tilt blocks of upper Paleozoic strata that lack close association with depositionally overlying tilted Tertiary rocks is even more uncertain. However, the folded Permian unit A–Ely Limestone contact near the northeast corner of sec. 30, T28N,R69E, southeast of White Horse Mountain, describes an east-dipping axial surface, which restored for steep westward tilting becomes west dipping, again suggesting east-vergent F_2 folding. Still other blocks, such as that west of the White Horse Mountain massif, when restored about a northerly tilt axis, have northeast-trending fold axes that may represent F_3 folds.

The time of displacement on the Ferguson detachment is not well constrained in the White Horse Pass area. However, the older Tertiary volcanic and clastic rocks in the hanging wall of the detachment in the southeast corner of the map area are steeply tilted, whereas horizontal rhyolite flows that have a fission-track age of 10.7±1.4 Ma and overlie near-vertical, tilted Pennsylvanian strata about 8 km north of Ferguson Mountain (see fig. 1) are reported by Ketner and others (1998). The Ferguson detachment is thus permissibly part of the widespread ~17 Ma extension event in east-central Nevada described by Miller and others (1999).

The Ferguson detachment is offset by high-angle basin-and-range normal faults that produced the modern topography in the region. One of these faults offsets the detachment in sec. 2, T29N,R69E and resembles the several similar north-northwest-trending high-angle faults mapped by Welsh (1994, fig. 1) farther to the north in the hills east of Ferguson Mountain. The White Horse Mountain massif is surrounded by exposed or inferred basin-and-range normal faults whose relatively downthrown sides face away from the mountain. One of these is the White Horse Pass fault that trends northwest through the pass. Down drop on this fault is to the northeast—uplifting the White Horse Mountain massif relative to the main Goshute Mountains. To the northwest of White Horse Pass, however, canyons draining the southwest flank of the main Goshute Mountains are conspicuously offset right laterally by about one-third of a kilometer across this fault. The northwest segment of the White Horse Pass fault thus was reactivated as a basin-and-range transform that accommodated the horizontal component of subsequent west-northwest dip-slip on the mountain-front faults along the northwest flank of the White Horse Mountain massif and those along the west side of the north-trending main Goshute Mountains farther to the northwest.

Followed south-southeast and then south from White Horse Pass, the trace of the White Horse Pass normal fault becomes obscure where it lies within the poorly exposed argillite member of the Chainman Shale (Mca) or is covered by older Quaternary gravels (Qo). When active, however, this poorly exposed to unexposed segment of the White Horse Pass fault east of the White Horse Mountain massif evidently produced a prominent scarp from which the coarse debris—including megabrecias—that characterize the more

western exposures of the Quaternary-Tertiary gravel (QTg) were derived. The apparent absence in this gravel of clasts representing units older than the Chainman argillite evidently results from the prevailing easterly dip of the footwall strata coupled with the extraordinary local thickness of the preserved Chainman argillite (cross section B–B′); only the Chainman argillite and the younger rocks in the hanging wall of the Ferguson detachment would have been exposed on the scarp despite its considerable (as much as 1 km) height.

Some basin-and-range normal faults postdate the White Horse Pass fault, but Holocene scarps are not apparent where these faults project through alluviated parts of the area or across the highstand shorelines of Pleistocene lakes in the area.

REFERENCES CITED

Allmendinger, R.W., and Miller, D.M., 1991, Modes of Late Jurassic intrusion and constraints on Jurassic & Cretaceous tectonics, western Utah and eastern Nevada: Geological Society of America Abstracts with Programs, v. 23, no. 5, p. A193.

Armstrong, R.L., 1970, K-Ar dating using neutron activation for Ar analysis—comparison with isotope dilation Ar analyses: Geochimica et Cosmochimica Acta, v. 34, p. 233–236.

Berge, J.S., 1960, Stratigraphy of the Ferguson Mountain area, Elko County, Nevada: Brigham Young University Geology Studies, v. 7, no. 5, p. 63.

Brooks, W.E., Thorman, C.H., Snee, L.W., Nutt, C.J., Potter, C.J., and Dubiel, R.F., 1995, Summary of chemical analyses and $^{40}Ar/^{39}Ar$ age-spectral data for Eocene volcanic rocks from the central part of the northeast Nevada volcanic field: U.S. Geological Survey Bulletin 1988-K, 33 p.

Coats, R.R., 1987, Geology of Elko County, Nevada: Nevada Bureau of Mines and Geology Bulletin 101, 112 p.

Crosbie, R.A., 1997, Sequence architecture of Mississippian strata in the White Pine Mountains, White Pine County, Nevada [M.S. thesis]: University of Nevada, Reno, 200 p.

Day, W.C., Elrick, M., Ketner, K.B., and Vaag, M.K., 1987, Geologic map of the Bluebell and Goshute Peak Wilderness Study Areas, Elko County, Nevada: U.S. Geological Survey Miscellaneous Field Studies Map MF-1932, scale 1:50,000.

Elison, M.W., 1995, Causes and consequences of Jurassic magmatism in the northern Great Basin: Implications for tectonic development, *in* Miller, D.M., and Busby, C., eds., Jurassic magmatism and tectonics of the North American Cordillera: Boulder, Colorado, Geological Society of America Special Paper 299, p. 249–265.

Epstein, A.G., Epstein, J.B., and Harris, L.D., 1977, Conodont color alteration—an index to organic metamorphism: U.S. Geological Survey Professional Paper 995, 27 p.

Gallegos, D.M., Snyder, W.S., and Spinosa, C., 1991, Tectonic implications of facies patterns, Lower Permian Dry Mountain trough, east-central Nevada, *in* Cooper, J.D., and Stevens, C.H., eds., Paleozoic paleogeography of the western United States-II: Pacific Section, Society of Economic Paleontologists and Mineralogists, v. 67, p. 343–346.

Hague, A., and Emmons, S.F., 1877, Descriptive geology: United States Geological Exploration of the Fortieth Parallel, v. II, 890 p.

Hintze, L.F., 1978, Sevier orogenic attenuation faulting in the Fish Spring and House Ranges, western Utah: Brigham Young University Geology Studies, v. 25, pt. 1, p. 11–24.

Karklins, O.L., Repetski, J.E., and Ketner, K.B., 1989, Maps showing ages and thermal maturation values of conodonts from the Goshute-Toana Range, Elko County, Nevada: U.S. Geological Survey Miscellaneous Field Studies Map MF-2065, scale 1:50,000.

Ketner, K.B., 1997, Geologic maps showing structural modes in the Goshute Mountains and Toana Range, Elko County, Nevada: U.S. Geological Survey Miscellaneous Investigations Map I-2546, scale 1:24,000.

Ketner, K.B., Day, W.C., Elrick, Maya, Vaag, M.K., Zimmermann, R.A., Snee, L.W., Saltus, R.W., Repetski, J.E., Wardlaw, B.R., Taylor, M.E., and Harris, A.G., 1998, An outline of tectonic, igneous, and metamorphic events in the Goshute-Toano Range between Silver Zone Pass and White Horse Pass, Elko County, Nevada: a history of superposed contractional and extensional deformation: U.S. Geological Survey Professional Paper 1593, 12 p.

Messin, G.M.L., 1973, Geology of the White Horse pluton, Elko County, Nevada [M.S. thesis]: University of Nebraska, Lincoln, 100 p.

Miller, D.M., 1990, Mesozoic and Cenozoic tectonic evolution of the northeastern Great Basin, *in* Shaddrick, D.R., Kizis, J.A., Jr., and Hunsaker, E.L., III, eds., Geology and ore deposits of the northeastern Great Basin: Geological Society of Nevada, Reno, p. 43–73.

Miller, D.M., and Hoisch, T.D., 1995, Jurassic tectonics of northeastern Nevada and northwestern Utah from the perspective of barometric studies, *in* Miller, D.M, and Busby, C., eds., Jurassic magmatism and tectonics of the North American Cordillera: Boulder, Colorado, Geological Society of America, Special Paper 299, p. 267–294.

Miller, E.L., Dumitru, T.A., Brown, R.W., and Gans, P.B., 1999, Rapid Miocene slip of the Snake Range-Deep Creek Range fault system, east-central Nevada: Geological Society of America Bulletin, v. 111, p. 886–905.

Misch, P., 1960, Regional structural reconnaissance in central-northeast Nevada and some adjacent areas: observations and interpretations, *in* Boettcher, J.W., and Sloan, W.W., Jr., eds., Guidebook to the geology of east central Nevada: Intermountain Association of Petroleum Geologists, Eleventh Annual Field Conference, p. 17–42.

Nichols, K.M., and Silberling, N.J., 1980, Eogenetic dolomitization in the pre-Tertiary of the Great Basin, *in* Zenger, D.J., Dunham, J.B., and Effington, R.L., eds., Concepts and models of dolomitization: Society of Economic Paleontologists and Mineralogists Special Publication 28, p. 237–246.

Nolan, T.B., 1935, The Gold Hill mining district, Utah: U.S. Geological Survey Professional Paper 177, 172 p.

Ponce, D.A., 1994, Aeromagnetic map of the east-central part of the Elko 1°x2° quadrangle, Nevada, *in* Thorman, C.H., Nutt, C.J., and Potter, C.J., eds., Dating of pre-Tertiary attenuation structures in upper Paleozoic and Mesozoic rocks and the Eocene history in northeast Nevada and northwest Utah: 1994 fieldtrip guidebook, Nevada Petroleum Society, Reno, p. 9–11.

Robinson, J.P., 1993, Provisional geologic map of the Gold Hill quadrangle, Tooele County, Utah: Utah Geological Survey Map 140, scale 1:24,000.

Silberling, N.J., and Nichols, K.M., 1994, Geometry of Tertiary low-angle detachment faulting controlled by earlier contractional structures, Goshute Range, Nevada: Geological Society of America Abstracts with Programs, v. 26, no. 6, p. 92.

Silberling, N.J., Nichols, K.M., Macke, D.L., and Trappe, J., 1995, Upper Devonian-Mississippian stratigraphic sequences in the distal Antler foreland of western Utah and adjoining Nevada: U.S. Geological Survey Bulletin 1988-H, p. H1–H33.

Silberling, N.J., Nichols, K.M., Trexler, J.H., Jr., Jewell, P.W., and Crosbie, R.A., 1997, Overview of Mississippian depositional and paleotectonic history of the Antler foreland, eastern Nevada and western Utah, *in* Link, P.K., and Kowallis, B.J., eds., Proterozoic to Recent stratigraphy, tectonics, and volcanology, Utah, Nevada, southern Idaho, and central Mexico [Geological Society of America, Field Trip Guidebook, 1997 Annual Meeting, Salt Lake City, Utah]: Brigham Young University Geology Studies, v. 42, pt. 1, p. 161–196.

Stacey, J.S., and Zartman, R.E., 1978, A lead and strontium isotopic study of igneous rocks and ores from the Gold Hill mining district, Utah: Utah Geology, v. 5, p. 1–15.

Steele, G., 1960, Pennsylvanian-Permian stratigraphy of east-central Nevada and adjacent Utah, *in* Boettcher, J.W., and Sloan, W.W., Jr., eds., Guidebook to the geology of east central Nevada: Salt Lake City, Intermountain Association of Petroleum Geologists, Eleventh Annual Field Conference, p. 91–113.

Thorman, C.H., Nutt, C.J., and Potter, C.J., 1994, Introduction to the 1994 Nevada Petroleum Society Fieldtrip, *in* Thorman, C.H., Nutt, C.J., and Potter, C.J., eds., Dating of pre-Tertiary attenuation structures in upper Paleozoic and Mesozoic rocks and the Eocene history in northeast Nevada and northwest Utah: 1994 fieldtrip guidebook, Nevada Petroleum Society, Reno, p. 1–2.

Van Wagoner, J.C., Posamentier, R.M., Mitchum, R.M., Vail, P.R., Sarg, J.F., Loutit, T.S., and Hardenbol, J., 1988, An overview of the fundamentals of sequence stratigraphy and key definitions, *in* Wilgus, C.K., and others, eds., Sea-level changes: An integrated approach: Society of Economic Paleontologists and Mineralogists, Special Publication 42, p. 39–45.

Welsh, J.E., 1994, Middle Jurassic tectonic plates: Ferguson Mountain, Elko County, Nevada, *in* Thorman, C.H., Nutt, C.J., and Potter, C.J., eds., Dating of pre-Tertiary attenuation structures in upper Paleozoic and Mesozoic rocks and the Eocene history in northeast Nevada and northwest Utah: 1994 fieldtrip guidebook, Nevada Petroleum Society, Reno, p. 87–94.

Zamudio, J.A., and Atkinson, W.W., Jr., 1992, Mesozoic deformation in the Dolly Varden Mountains and Currie Hills, Nevada: Geological Society of America Abstracts with Programs, v. 24, p. 69.

GEOLOGIC MAP OF THE WHITE HORSE PASS AREA, ELKO COUNTY, NEVADA

N.J. SILBERLING AND K.M. NICHOLS

2002

SURFICIAL DEPOSITS AND CENOZOIC ROCKS

Qa **Quaternary alluvium** Unconsolidated alluvial deposits in major active drainages. Also includes sheet-wash deposits of coarse-grained granitic sand derived from the White Horse pluton that overlap the highstand Quaternary lacustrine deposits at the edge of Antelope Valley.

Qd **Quaternary sand-dune deposits** Unconsolidated, well-sorted, wind-blown sand concentrated in several patches southwest of White Horse Pass.

Qb **Quaternary lacustrine bar deposits** Poorly consolidated fine- to medium-gravel forming the conspicuous bar paralleling the highstand level of Pleistocene Lake Bonneville northward from Ferber Wash. Evidently formed by interaction between the highstand of Lake Bonneville and the sediment load from Ferber Wash, whose drainage basin within the map area and to the south and southeast is about 145 km^2.

Ql **Quaternary lacustrine deposits** Fine-grained lacustrine deposits and redeposited older alluvium locally forming minor beaches and bars associated with Lake Bonneville and the Pleistocene lake that occupied Antelope Valley. Inconspicuous except on aerial photographs.

Qo **Quaternary older alluvium** Alluvial fan deposits predating the highstands of Lake Bonneville and the Pleistocene lake in Antelope Valley; also thick, extensive talus and associated alluvial deposits in mountain valleys.

Qt **Quaternary tuff** Loosely consolidated, massive pumiceous tuff having a maximum thickness of a few meters. Contains layers of reworked tuffaceous sediment containing gravel; appears to be in the lowermost part of unit "Qo." Shown only where observed along the edge of White Horse Flat in the east-central sec. 20 and west-central sec. 29, T28N, R69E, and S½ sec. 10, T29N, R69E.

QTg **Quaternary-Tertiary gravel** Poorly sorted sedimentary breccia and gravel containing clasts up to several meters in long dimension. Partly to completely indurated. Matrix poor where best exposed in western part of outcrop area. Clast composition varies according to underlying rocks, so that in more western exposures recognizable clasts represent the Ely Limestone (IPe) and quartzite of the argillite member of the Chainman Shale (Mca); clasts in eastern exposures include fusulinid limestone derived from Permian unit A (PA) and igneous rocks from the Tertiary andesite unit (Ta). Distinctive clasts from units older than the argillite unit of the Chainman Shale (Mca), such as the Needle Siltstone Member of the Chainman Shale (Mcn) or the Guilmette Formation (Dg), were not observed. Although essentially unbedded and lacking in fluviatile deposits, at least in the more western and better exposed outcrops, crude layering results from differences in clast composition. In the low-relief, more eastern exposures, the light and dark bands apparent on aerial photographs are layers rich in limestone and in Tertiary andesitic rocks, respectively. Unit is confined to a 5-km-long band of outcrops in the low hills west of White Horse Mountain. Layering, as viewed on aerial photographs or from the distance, consistently dips 5-10° to the southeast. Exposed thickness exceeds 100 m.

Tr **Tertiary rhyolitic tuff** Vitroclastic rhyolitic tuff and flow-banded rhyolite containing conspicuous phenocrysts of biotite and less abundant white feldspar and quartz. Vitrophyric basal part of unit conspicuously perlitic in part. Unit is poorly exposed and confined to central sec. 35, T28N, R69E. Maximum exposed thickness about 300 m.

Tg **Tertiary gravel** Well-layered, steeply dipping gravel containing clasts up to boulder size derived both from the underlying Tertiary andesite unit and from pre-Tertiary rocks such as Permian limestone. No outcrops of this gravel were observed, but areas underlain by its surficial weathered debris are readily separated from areas of the compositionally similar, locally overlying, Quaternary older gravel by the regular, steep layering conspicuous on aerial photographs. Appears to concordantly overlie the Tertiary andesite unit (Ta). Apparent thickness at least several hundred meters but could be internally faulted. Confined to the southeast corner of the map area.

Ta **Tertiary andesite** Mainly dark agglomeratic andesite lahar deposits and interstratified andesite flows. Flow-banded dacite observed in a single outcrop just above the apparent base of the unit where it is interpreted to rest depositionally on red-stained (weathered?) limestone of unit Px (east-central sec. 34, T28N, R69E). Outcrops rare except in larger stream courses. Interstratified volcaniclastic fluviatile gravel observed in cut-bank exposures at one place (central sec. 26, T28N, R69E). Unit may be repeated by unrecognized faults, but it is at least several hundred meters thick. Restricted to the southeast corner of the map area, where it is part of a broad belt of older Tertiary andesitic rocks included by Coats (1987) in his unit "Ta," and shown by him as extending westward, south of the present map area, for about 50 km. Age probably Eocene; scattered, small outcrops of dacite having $^{40}Ar/^{39}Ar$ age of 39.80±0.1 Ma (Brooks and others, 1995) overlie unit PC as close as 16 km to the north of unit Ta exposures and 2 km north of the northeast corner of the White Horse Pass map area.

CENOZOIC OR MESOZOIC ROCKS

d **Dike rocks (Undated)** Dike rocks of silicic to intermediate composition and having granitic textures; mostly extensively altered. Although some of the mapped dikes are assigned a Tertiary age by Day and others (1987) and by Welsh (1994), most of these parallel or intrude pre-Tertiary faults or else they are sills that are folded along with the enclosing pre-Tertiary strata, and they are thus more likely Mesozoic—probably Jurassic—in age.

MESOZOIC ROCKS

Jg **Granitic rocks of the White Horse pluton (Upper Jurassic)** Granitic rocks ranging in composition from quartz-poor granodiorite to quartz-rich granite, but consisting predominantly of medium-grained, seriate-porphyritic quartz monzonite according to Mesain (1973), as paraphrased by Coats (1987). $^{40}K/^{40}Ar$ age on hornblende and biotite of 158±3 Ma reported by Armstrong (1970), recalculated as ca. 160 Ma (Miller and Hoisch, 1995). Geochemical, isotopic, and geobarometric data and interpretation given by Miller and Hoisch (1995).

TrT **Thaynes Formation (Lower Triassic)** Yellow-gray weathering, platy-parting, calcareous siltstone intergradational with nodular impure limestone. Restricted to a single exposure at the north margin of the map area (north-central sec. 4, T29N, R69E).

PALEOZOIC ROCKS

Permian strata

Permian strata in the White Horse Pass area and immediately to the north, at and near Ferguson Mountain, have customarily been assigned, in ascending order, to the Ferguson Mountain Formation, Pequop Formation (or Arcturus Formation), Loray Formation (sometimes included in the Pequop or Arcturus Formations), Kaibab Limestone, Plympton Formation (usually including or treated as an equivalent of the Phosphoria Formation), and Gerster Limestone (Berge, 1960; Steele, 1960; Coats, 1987; Gallegos and others, 1991; and Welsh, 1994). Equivalents of the Gerster and much of the Plympton were not observed in the map area. Among the other units, discounting assignments based on interpreted age or regional correlations, the lithologic basis for separating the various formations is for the most part vague. Neither sedimentologically based stratigraphic study nor detailed maps (other than that by Berge, 1960, which locates the upper and lower boundaries of his Ferguson Mountain Formation on Ferguson Mountain) are available to aid in recognizing the successive named units. Revision of the Permian stratigraphy, utilizing modern concepts such as sequence stratigraphy, would necessarily include exposures outside the present map area and is beyond the scope of the present study. For these reasons, Permian strata in the White Horse Pass area are assigned to utilitarian map units designated simply as Permian unit A, unit B, and unit C.

For characterization of the Permian units and the other, older carbonate rock units in the map area, the concepts and terminology of sequence stratigraphy are regarded as essential in a descriptive sense. For an explanation of sequence stratigraphy see, for example, Van Wagoner and others (1988).

Pc **Permian unit C** Dolostone and limestone. Mostly coarsely crystalline eogenetic secondary dolostone; some limestone preserved locally near base. Lower part of unit C contains several meters of continuous, resistant, mainly medium-thick chert layers that form cuesta-like exposures. Evaporitic dolomudstone observed in one place relatively high in unit. Large productid brachiopods near base and silicified shell fragments higher in section attest to more open-marine deposition than the underlying supratidal rocks of Permian unit B; the base of unit C thus represents a stratigraphic sequence boundary. Among the stratigraphically highest rocks of unit Pc is poorly exposed dark sandstone cropping out at one place on north side of Dead Cedar Wash (NW¼ NE¼, sec. 4, T29N, R69E). At least the lower part of unit C corresponds to the Kaibab Limestone as recognized in the area by previous authors. Higher parts of the unit may correspond to their Plympton Formation. Exposed thickness exceeds 100 m. Within the map area crops out only in the Ferguson Mtn. Quadrangle.

Ps **Permian unit B** Dolomudstone and sandstone. From scattered outcrops and float, unit includes evaporitic dolomudstone, impure dolomudstone, and dolomitic siltstone or fine-grained sandstone. Poor exposure of unit B within the map area precludes observing the stratigraphic succession of the different rock types. Fine-grained sedimentary breccias composed of dolomudstone and the occurrence of chalcedony nodules and stringers within dolomudstone indicate original presence of evaporites; gypsum is reported nearby at Ferguson Mountain (Berge, 1960). Some dolomudstone is microbially laminated. Dolomitic siltstone or sandstone is either massive or herringbone cross-stratified on a small scale. Unit B is interpreted as a supratidal and tidal-flat deposit. Maximum estimated thickness about 200 m. Unit corresponds to the Loray Formation or part of the Arcturus Formation as applied previously in or near the map area. Permian unit B crops out only in the part of the Ferguson Mtn. Quadrangle included within the map area.

PA **Permian unit A** Limestone, sandstone, and dolomudstone. Permian unit A is a thick succession that is incomplete everywhere within the map area and contains repetitive lithologic units such as cherty massive limestone. Consequently, its characterization is both complicated and partly interpretive. It consists of peritidal cyclic parasequences ranging from a few to a few tens of meters in thickness. Basal parts of parasequences are massive, cliff-forming, commonly cherty, limestones overlain by more thinly and well-bedded limestones which in the more heterogeneous parasequences are in turn overlain by impure limestone, calcareous siltstone and fine-grained sandstone, or lime mudstone and dolomudstone, some of which is microbially laminated. Massive limestone units are mainly bioclastic packstones and wackestones. Many lack conspicuous crinoidal bioclasts, although crinoidal grainstones and packstones form part or all of some massive limestone units. In the overlying bedded limestone, impure limestone, and calcareous sandstone, fusilinids are common, in places occurring in rock-forming abundances.

The apparently most complete section of unit A within the map area is exposed in the hills a few kilometers southeast of White Horse Mountain. Here, unit A overlies the Ely Limestone, but its upper part is not exposed.

This section includes one complete third-order stratigraphic sequence and the lower part of another, the sequence boundary within unit A being at about the 6600-foot topographic contour east of elevation point 6743 on the crest line of these hills. The lower sequence is about 650 m thick and is distinguished from the higher in having supratidal desiccated lime mudstone or dolomudstone at the tops of individual parasequences. Within the bedded limestones, above the massive, basal limestones of the parasequences, ramose bryozoan fossils, occasionally associated with brachiopod shells, commonly occur in beds stratigraphically lower than those containing fusilinids, which occur to the exclusion of other megascopic fossils. Within the intra-parasequence succession of rock types, fusilinids thus evidently characterize the most evaporitically restricted fossiliferous rocks. Higher parts of the parasequences are unfossiliferous, partly supratidal deposits. In the lower part of the lower sequence within unit A, massive chert-stringer limestones, commonly crinoidal grainstones and packstones, tend to predominate the section; higher and near the top of the sequence massive limestones are thinner and non-bioclastic impure carbonate rocks and pale yellowish-gray dolomudstones attain thicknesses of 5 to 10 m in some parasequences. The lower sequence within unit A apparently is preserved only in the hills east and southeast of the White Horse Mountain massif where it overlies the Ely Limestone which forms the lower part of the hanging wall of the Ferguson detachment fault (see accompanying text).

In the overlying, incompletely exposed, upper third-order sequence within unit A, massive, more or less cherty, partly bioclastic gray limestones forming the lower parts of the included parasequences are characteristically separated by intervals of grayish-orange to yellowish-brown, commonly fusilinid bearing, fine-grained calcareous sandstone or impure limestone. Solitary or colonial corals occur sporadically in the massive bioclastic limestone units. Where exposed within the map area above the Ely Limestone in the hills southeast of White Horse Mountain, less than 100 m of this upper sequence is exposed. However, in the Ferber Hills and in the part of the map area within the Ferguson Mtn. Quadrangle, where unit A directly overlies the Ferguson detachment (see text), most of unit A apparently consists of the upper sequence, partial sections of which exceed 1,000 m in thickness if not repeated by unrecognized faults. The upper sequence of unit A, together with Permian unit B, may define a complete third-order stratigraphic sequence. The total thickness of Permian unit A probably exceeds 1,500 m. The unit corresponds to the rocks in the general area assigned to the Ferguson Mountain, Pequop, and Arcturus Formations by previous authors.

IPe **Ely Limestone (Pennsylvanian)** Limestone, sandy limestone, quartzite, and dolomudstone. A peritidal cyclic succession dominated by units of massive, more or less cherty, limestone that form the lower parts of parasequences. The limestone units are commonly crinoidal grainstones or crinoid-bioclast packstones and wackestones, except in the stratigraphically higher parts of the Ely where massive units of lime mudstone or sparsely bioclastic lime wackestone prevail. Many of the limestones contain quartz sand or are streaked with quartz sand, exhibiting conspicuous, centimeter-scale, tabular cross-stratification. Some massive limestones grade up into fine- to medium-grained calcareous sandstone or, locally, quartzite in units up to 12 m thick. Less sandy parasequences may be capped with desiccated lime mudstone or dolomudstone, some of which is microbially laminated.

Compared to the equally cyclic and lithologically similar Permian unit A, the Ely Limestone is differentiated by having more abundant crinoidal grainstones, more and coarser quartz sand as a component of the limestones or as discrete units, larger scale cross-stratification in the lower parts of the parasequences, and in general having the aspect of more open marine and energetically deposited strata. Megascopically recognizable fusilinids were not observed in the Ely Limestone. The maximum exposed thickness of the Ely within the map area is 800-1,000 m.

Chainman Shale (Mississippian)

The Chainman Shale within the map area is divided into four lithologically distinct members, in descending order, the: argillite member, siltstone member, White Horse Pass limestone member, and the Needle Siltstone Member. Apparently complete sections of the White Horse Pass limestone and Needle Siltstone members are locally preserved, but where the siltstone member is preserved at all within the map area, its upper contact is an attenuation fault. The internally much deformed argillite member is bounded below by this same attenuation fault and above by the Ferguson detachment fault; locally it is completely cut out beneath the Ferguson detachment.

Mca **Argillite member** The argillite member is preponderantly highly fractured black or very dark olive-gray argillite. In most places bedding is expressed only by occasional, discontinuous, thin interbeds of yellowish brown dolomitic sandstone or quartzite, or more rarely of dark, impure, dense limestone. Boldly outcropping packets of medium- to thick-bedded, light brownish-gray quartzite occur locally, in the structurally, if not stratigraphically higher parts of the unit. Quartzite beds commonly have tabular cross-stratification and are current rippled on their top surfaces. Most of the bedding and minor-fold attitudes shown for the argillite member on the map are those of quartzite beds.

The argillite unit forms an internally deformed mass between the Mesozoic attenuation fault at its structural base and the Tertiary-Ferguson detachment fault; neither the stratigraphic top nor bottom of the member is preserved. The structural thickness of the argillite member varies from 0 to several hundred meters within the map area.

Mcs **Siltstone member** The siltstone member is restricted to stratigraphically thin exposures that crop out locally beneath the attenuation fault at the structural base of the argillite member of the Chainman Shale. North of White Horse Pass it consists of up to several meters of pale-red to light brown, platy to slabby weathering calcareous siltstone bearing abundant bedding-parallel, irregularly sinuous, feeding tracks. Where the preserved thickness of the member is greatest, about 3 km southeast of White Horse Pass, it is internally folded, cut by thin dikes, and poorly exposed. Here, its maximum thickness is only a few tens of meters, and in addition to yellow-brown, pale-red, and gray calcareous siltstone it contains some laminated siliceous shale and a few isolated beds of lime mudstone. At one place, float of a silicified, coarse-grained, phosphorite lag deposit, probably no more than several centimeters thick, occurs well above the base of the member.

Mcw **White Horse Pass limestone member** The major part of this member is regularly medium- to thick-bedded, internally featureless lime mudstone characteristically weathering to medium dark gray (N4 of the Geological Society of America Rock-Color Chart). Bed partings within the limestone are distinct and marked by siliciclastic impurities or thin intercalations of yellow-brown to pale-red calcareous siltstone. Rarely, up to a few meters of calcareous siltstone or slabby weathering impure limestone are interbedded with the ubiquitous lime mudstone. Near or at the base of the member are one or two beds, up to 1.5 m thick, of crinoidal grainstone, some of which display dune-like cross stratification having generally southward sloping foresets after bedding is restored to horizontal. The stratigraphically highest 10 m or so of the member is also characterized by drifts of crinoidal bioclasts on the surfaces of lime-mudstone beds and by beds of crinoidal packstone and grainstone. The lime mudstone forming the bulk of the member commonly contains conspicuous anastomosing, solution(?) cleavage surfaces having sub-millimeter spacing. This cleavage mostly parallels bedding. Maximum structural thickness of the internally deformed White Horse Pass limestone member is about 100 m.

The limestone of White Horse Pass, as informally named by Day and others (1987), is equivalent to the Ochre Mountain Limestone of Nolan (1935) in the Gold Hill mining district about 30 km east of the White Horse Pass map area. However, this prior name is not used herein because the typical example of the Ochre Mountain is not only intensely fractured, but also pervasively dolomitized and silicified, making lithologic comparison uncertain. Aside from its altered nature, the Ochre Mountain also appears to be more crinoidal within the main body of the unit and to contain less intercalated siltstone than does the White Horse Pass limestone. Welsh (1994) assigned the member to the Camp Canyon Limestone, another correlative but lithologically distinct unit in westernmost Utah.

Mcn **Needle Siltstone Member** Platy to flaggy weathering, dolomitic or calcareous siltstone and very fine-grained sandstone, characteristically light brown to yellowish orange, more rarely pale red weathering. Locally, especially relatively low in the section, bedding-parallel, irregularly sinuous burrows are abundant. Dolomite is entirely secondary in subhedral to euhedral crystals which may constitute more than half the rock volume, in which case the dolomitic siltstone grades into silty dolostone. In addition to 50-100 µm quartz grains, detrital minerals include a few percent of feldspar and mica. Obliately spheroidal phosphatic nodules occur sparsely throughout the unit.

Most of the Needle Siltstone within the map area has an attenuation fault essentially at its base. Near the base, float of peloidal phosphorite beds up to 2 cm thick, black chert, gray platy mudstone, and lime mudstone are characteristic. Where the member rests depositionally on the Joana Limestone, a 0.5 m-thick bed of featureless lime mudstone crops out several meters above the base. East of White Horse Mountain, where the Needle Siltstone section is complete, its thickness is about 100 m.

The Needle Siltstone in the map area is equivalent to the Woodman Formation of Nolan (1935), named in the Gold Hill mining district about 30 km to the east. Despite the priority of Nolan's name, the unit is referred herein to the better-known Needle Siltstone Member, following the usage of Day and others (1987) in the White Horse Pass area. The basal phosphatic part of the member is recognized as a separate unit beneath Needle Siltstone and referred to as the "Delle member" by Welsh (1994), but regionally there is no consistent means of recognizing a lithic boundary between the Delle and Needle members away from the type section of the Delle in north-central Utah.

Joana Limestone (Mississippian)

The Joana Limestone is divided into an upper and a lower member, but because of attenuation faulting, no continuous section of them occurs in the map area. Along the east margin of White Horse Mountain, the attenuation fault that separates the two members of the Joana progressively cuts out the lower member in its footwall as it is traced southwestward. Farther north, the upper member is completely removed from the hanging wall of this same fault.

Mju **Upper member (Lower Mississippian)** Evenly and rythmically medium-bedded, medium dark-gray limestone. Commonly conspicuously crinoidal, but ranging from crinoidal grainstone to lime mudstone. Fine-grained beds characteristically have siliciclastic impurities and crinoidal bioclasts on parting surfaces of bedding. Bedding normally graded in part. Interpreted as a tempestite, i.e., a deep-subtidal storm deposit. The upper member of the Joana along the southwest flank of White Horse Mountain is largely or wholly replaced by jasperoid.

The upper member of the Joana in the map area generally resembles the upper member of the *nectrys* Joana Limestone at Ward Mountain in the Egan Range and the "Harris Canyon member" of the Joana of Crosbie (1997; Silberling and others, 1997), named for exposures in the Schell Creek Range.

Mjl **Lower member (Lower Mississippian)** Mostly massive, solution-compacted, neomorphosed limestone having thick stylolitic parting. Sparse crinoidal bioclasts preserved locally; dense limestones appear to have been pellet-calcisphere wackestones and packstones, some of which are faintly mottled. Rare megafossils include large gastropods and, in one place, solitary corals. Oncolites occur at two levels in the lower Joana east of Sugar Loaf Peak. Here, the lowest few meters of the member retain some of the rhythmically thin- and medium-bedded character distinctive of the basal lithosome (unit MO.Rh.Lm of Silberling and others, 1995) of the Joana regionally, and these beds rest depositionally on the Guilmette Formation. North of White Horse Pass the basal meter or so of the Joana is planar-laminated limestone, and the contact with the underlying Guilmette is a karst surface having more than a half meter of relief. This is especially well displayed in the west-central NW¼ sec. 24, T29N, R68W. Conodonts recovered from two samples collected at about the same stratigraphic level within the lower Joana in the E½ sec. 26, T29N, R69W range in age from early Famennian to Kinderhookian (R.G. Stamm, written commun., 1994) and are evidently largely reworked from strata that were eroded prior to deposition of the Joana unconformably upon the Guilmette Formation.

Dg **Guilmette Formation (Devonian)** Limestone, dolostone, and quartzite. A cliff-forming succession of shallowing-upward, peritidal cycles or parasequences, each a few meters to tens of meters in thickness. The component rock types within the parasequences vary through the section, but an idealized complete parasequence contains from the bottom upwards: (1) dark gray limestone, some of which contains low-diversity shelly faunas of pelecypods, gastropods, or brachiopods; (2) gray limestone containing rounded heads of stromatoporoids up to 20 cm in diameter; (3) gray limestone containing spaghetti-like masses of the coelenterate *Amphipora*; (4) gray lime mudstone or beds of fossils but locally streaked and mottled with brown-gray weathering impure dolostone; and (5) light-gray-weathering dolomudstone ("penecontemporaneous" dolostone), some of which has microbial lamination or, more rarely, low-amplitude stromatolites. Some parasequences are mainly dolomitic, whereas others are primarily composed of limestone. White to light brown dolomitic quartzose sandstone or quartzite in units up to 20 m thick occurs sparsely in the dolostones or above them, in which case they cap the parasequences. Quartzite is more conspicuous in the lower part of the Guilmette as exposed. Some of the thicker quartzite units, or sets of quartzite units in successive parasequences are traceable for several kilometers, but most quartzite units are laterally discontinuous. The original limestones forming the lower parts of parasequences may be replaced with featureless, light-gray to white, sugary, secondary dolostone, for the most part apparently of eogenetic (Nichols and Silberling, 1980) replacement origin.

In the isoclinally folded Guilmette marble within the contact zone of the White Horse pluton, the strongly asymmetric succession of different rock types forming the peritidal parasequences provides a reliable top vs. bottom criterion, along with preferred orientation of shelly fossils according to shape and geopetal deposits within bivalve and gastropod shells. Variation in the relative representation of the different rock types within cycles, and trends of systematic variation in cycle thicknesses, suggest that more than one third-order stratigraphic sequence is represented by the exposed part of the Guilmette Formation. Maximum exposed thickness is only several hundred meters; much of the lower part of the formation is not exposed within the map area.

See accompanying text for references and a description of the structural evolution of the map area.

QUATERNARY — Qa, Qd, Ql, Qb, Qo, Qt

TERTIARY — QTg Depositional on Ta, PA, and IPe; Tr; Tg; Ta Depositional on PA within map area

JURASSIC — d; Jg Intrudes Dg

TRIASSIC — TrT

PERMIAN — Pc; Ps; PA

PENNSYLVANIAN — IPe

Ferguson detachment fault

MISSISSIPPIAN — Mca; *Attenuation fault*; Mcs; Mcw; Mcn; Miju; *Attenuation fault*; Mjl

DEVONIAN — Dg

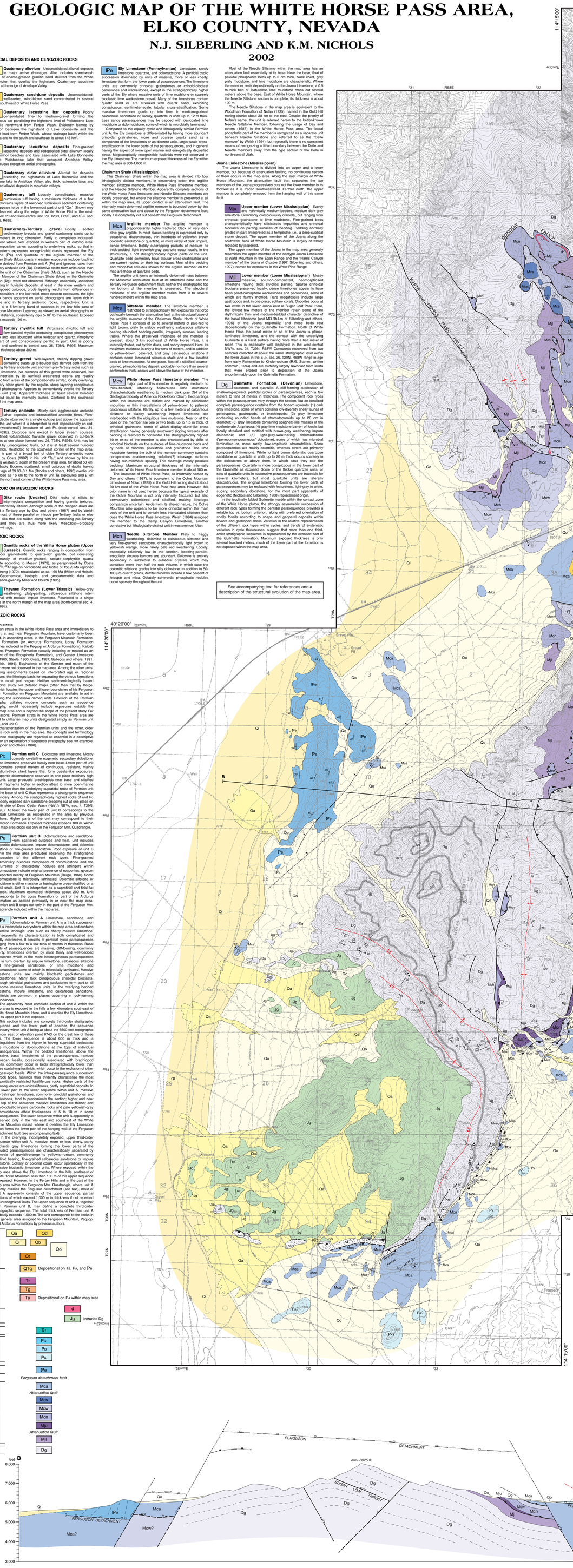

Contact Dashed where approximately located.

Trace of bedding Shown locally for structural control.

Projection of bedding above ground level On cross section B-B'.

Normal fault Dashed where approximately located; dotted where concealed on map or projected above ground level on cross sections; bar and ball on downthrown side; arrow indicates measured dip.

Strike-slip fault Dashed where approximately located; dotted where concealed.

Ferguson detachment fault Dashed where approximately located; dotted where concealed on map or projected above ground level on cross sections; open rectangles on hanging wall.

Dondon low-angle normal fault Dashed where approximately located; dotted where concealed. Ticks on hanging wall.

Mesozoic attenuation fault Dashed where approximately located; dotted where concealed on map or projected above ground level on cross sections; solid rectangles on upper plate.

Thrust fault Dashed where approximately located; dotted where concealed; barbs on upper plate.

Axial traces of F_1 folds showing plunge Anticline, syncline, overturned anticline, and overturned syncline. Arrows indicate dip of limbs.

Axial traces of F_2 and F_3 folds Dip symbols as with F_1 folds.

Jasperoid Replacement of carbonate rocks, mainly those of Miju. Labelled Miju where remnants of this unit are preserved.

Sill swarms Propylitized granitic-textured sills too thin to be mapped separately. Where exposures of these sills are sufficiently large to show on map, they are assigned to unit d.

Strike and dip of beds Inclined, overturned, vertical, and horizontal.

Strike and dip of beds Facing direction, as marked by ball, determined from depositional features; inclined, overturned, and vertical.

Strike and dip of beds Generalized where variable and estimated from aerial photographs; inclined and vertical; facing direction marked by ball.

Strike and dip of flow banding in Tertiary volcanic rocks Inclined and generalized where variable.

Strike and dip of solution-cleavage foliation in Mcw and grain-shape foliation in Dg Inclined and vertical.

Strike and dip of bedding and foliation coincident Foliation in plane of bedding; inclined, overturned, and vertical.
Inclination of foliation and bedding different; bedding vertical, facing direction marked by ball.

Strike and dip of fracture cleavage Inclined, vertical.

Plunge of elongation lineation May be combined with symbols for foliation or bedding.

Strike and dip of planar veins Inclined and vertical. Multiple, planar, parallel calcite veins interpreted as flexural-extension features parallel to axial surfaces of F_2 or F_3 folds.

Trend on bedding surface of en echelon calcite-vein gash array Plane parallel to gash array roughly orthogonal to gently dipping bed; arrow shows sense of shear.

Trends on bedding surface of conjugate en echelon calcite-vein gash arrays Intersection of planes parallel to arrays interpreted as the Y axis of flexural-extension strain ellipsoid. Sense of strike-slip then defines extensional (X) and contractional (Z) directions of flexural extension.

Trend and plunge of minor folds Anticline, syncline, multiple, and horizontal.

Trend and plunge of fold axis and dip and strike of axial surface Plunge of axis inclined, horizontal.

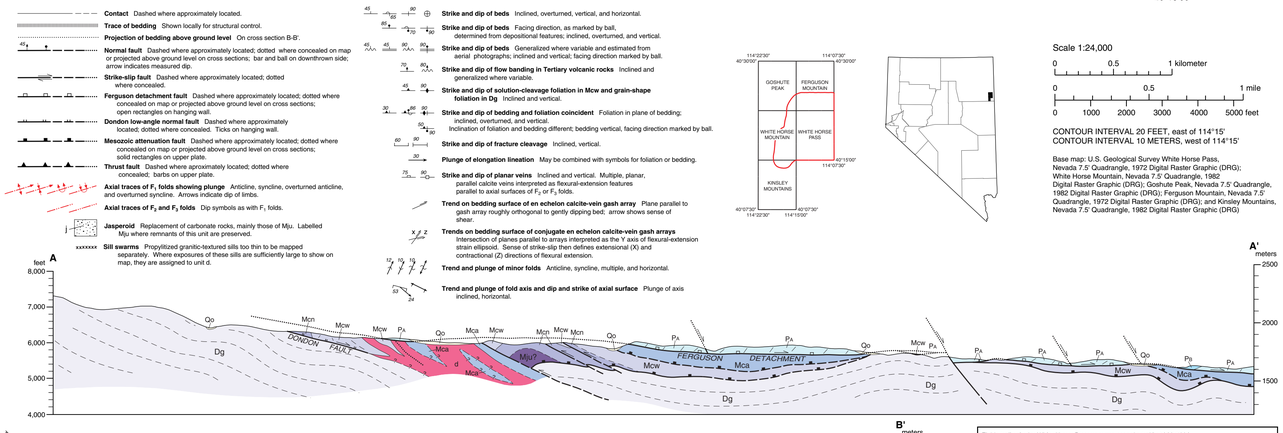

Scale 1:24,000

0 0.5 1 kilometer

0 0.5 1 mile

0 1000 2000 3000 4000 5000 feet

CONTOUR INTERVAL 20 FEET, east of 114°15'
CONTOUR INTERVAL 10 METERS, west of 114°15'

Base map: U.S. Geological Survey White Horse Pass, Nevada 7.5' Quadrangle, 1972 Digital Raster Graphic (DRG); White Horse Mountain, Nevada 7.5' Quadrangle, 1982 Digital Raster Graphic (DRG); Goshute Peak, Nevada 7.5' Quadrangle, 1982 Digital Raster Graphic (DRG); Ferguson Mountain, Nevada 7.5' Quadrangle, 1972 Digital Raster Graphic (DRG); and Kinsley Mountains, Nevada 7.5' Quadrangle, 1982 Digital Raster Graphic (DRG)

Field studies in the White Horse Pass map were conducted in 1989-1998.

Office Review by: Phyllis A. Camilleri (Austin Peay University), Christopher D. Henry (NBMG), and A. Elizabeth Jones-Crafford (GeoLogic Services).

Field Review by: Christopher D. Henry (NBMG), and A. Elizabeth Jones-Crafford (GeoLogic Services).

First edition, first printing, 2002
Printed by Nevada Bureau of Mines and Geology, Reno, Nevada
Edited by Dick Meeuwig; cartography by Robert Chaney

Geologic mapping was mainly supported by the Geological Society of Nevada. Initial mapping in the area was carried out as part of a larger study of rocks of the Antler foreland partially supported by the U.S. Geological Survey. Interpretation of the White Horse Mountain area was aided by a copy of a small-scale preliminary map provided by R.W. Allmendinger. Insight into the geology of the Ferguson Mountain Quadrangle was gained from a Nevada Petroleum Society field trip led by J.E. Welsh in 1994.

Nevada Bureau of Mines and Geology
University of Nevada, Mail Stop 178
Reno, Nevada 89557-0088
(775) 784-6691, ext. 2
www.nbmg.unr.edu; nbmgsales@unr.edu